Single-Chain and Aggregation Properties of Semiconducting Polymer Solutions Investigated by Coarse-Grained Langevin Dynamics Simulation

Cheng K. Lee,[†,‡] Chi C. Hua,*[,†] and Show A. Chen[§,||]

Department of Chemical Engineering, National Chung Cheng University, Chia-Yi 621, Taiwan, R.O.C., and Department of Chemical Engineering, National Tsing Hua University, Hsin-Chu 30013, Taiwan, R.O.C.

Received: September 2, 2007; Revised Manuscript Received: July 18, 2008

A coarse-grained (CG) model and Langevin dynamics scheme are proposed to investigate the material properties in dilute solution of a model semiconducting conjugated polymer, poly(2-methoxy-5-(2′-ethylhexyloxy)-1,4-phenylenevinylene) (MEH-PPV). While the intra- and intermolecular potentials for the CG particle (currently, a monomer unit) were determined from the molecular dynamics (MD) simulation of a united atomistic model, fluctuation−dissipation forces arising from the treatment of a solvent field were self-consistently constructed from the measured particle diffusivity in a given solvent (i.e., chloroform or toluene) through the atomistic MD simulation. It is shown that the resultant Langevin dynamics simulation, which is substantially more efficient than the counterpart MD simulation of the same CG model, is able to capture the dynamic (such as center-of-mass diffusivity) as well as the structural (such as radius of gyration) features of the investigated polymer solutions. Essential material properties that can now be directly studied include the following: Scaling exponents for estimating the exact solvent qualities were, for the first time, determined for the two solvent systems investigated; the persistence length obtained was also noted to be in excellent agreement with early experimental estimations. Preliminary observations on the supramolecular aggregation properties were in good agreement with the general observations from a wide range of recent experiments, and shed light on the essential impact of solvent quality on the supramolecular aggregation structures.

1. Introduction

Conjugated polymers, such as poly (*p*-phenylenevinylene) (PPV) and its derivatives, have recently received widespread interest because of their potential application in fabricating polymer-based light-emitting diodes.[1] For its ability to dissolve in many organic solvents, MEH-PPV has become one of the most commonly studied conjugated polymers.[2] There are, however, many factors that have been recognized to affect the electrical/optical properties of the polymer diodes fabricated from it. In particular, it has frequently been demonstrated that the optical properties of MEH-PPV solutions or spin-cast films can be modified substantially by the presence of polymer aggregates, originally formed in solution and subsequently carried into the film through the casting process.[3−10] Therefore, it is of scientific and technological importance to understand the material properties in MEH-PPV solutions.

Understanding the aggregation properties in MEH-PPV solutions has relied mainly on experimental characterizations, including spectroscopic analyses[4,5,9] (e.g., UV−vis adsorption and photoluminescence, PL), small-angle neutron/X-ray scattering (SANS/SAXS),[9,10] and viscometric measurements[11] etc. Moreover, a few molecular[12−14] or Brownian[15] dynamics simulations have been carried out to shed light on previous experimental observations. Overall, these studies have consistently revealed a generally important impact of solvent quality on the aggregation properties of MEH-PPV solutions. It is of interest to note, however, that the exact solvent qualities for commonly studied MEH-PPV solution systems have never been reported, and, in particular, their impact on the supramolecular aggregation properties remains largely unexplored. An important reason for this is that the solvent quality of a polymer solution has typically been evaluated from single-chain (such as the coil size) or associated solution (such as the intrinsic viscosity) properties, yet a great tendency for MEH-PPV chains to form aggregates in essentially all solvents known prevents related data from being obtained in practice. These observations have motivated the present simulation study, which, in turn, was encouraged by the recent advance in coarse-grained (CG) simulations, as we briefly introduce below.

Recently, there has been a significant proliferation of researches taking advantage of CG models and simulation schemes to gain insights into the structural and even dynamic features in complex fluid systems.[15−31] In general, a CG model is established on the basis of the easily accessible, yet computationally more expensive, atomistic model and its molecular dynamics (MD) simulation. Essential information obtained from an atomistic MD simulation usually includes the Boltzmann trajectories of properly redefined bond lengths or angles[17,20] as well as the radial distribution functions (RDFs) for the particles in the CG model. The previous MD data can, in principle, be utilized to reconstruct the force fields in the CG model, and typically a similar MD simulation was then performed to study larger-scale material properties. The above procedures ensure that the structural features of primary interest may be captured in a self-consistent and more efficient manner. Along with an additional fitting procedure for essential time constants, the dynamic properties can also be inferred (see, for example, ref 24 for a recent review).

The strategies and simulation scheme outlined above for constructing a CG model, in general, suffer from the difficulty

* Corresponding author. E-mail: chmcch@ccu.edu.tw.
† Department of Chemical Engineering, National Chung Cheng University.
‡ E-mail: cklee@alumni.ccu.edu.tw.
§ Department of Chemical Engineering, National Tsing Hua University.
|| E-mail: sachen@che.nthu.edu.tw.

10.1021/jp077054g CCC: $40.75
Published on Web 08/26/2008

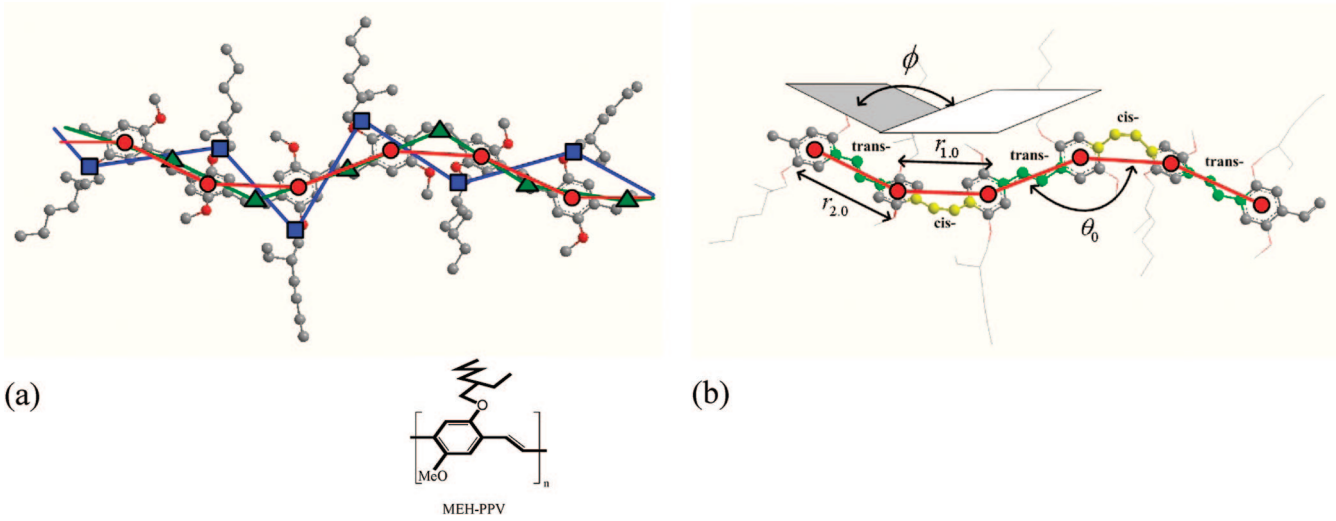

Figure 1. (a) Representations of an alternating cis−trans MEH-PPV chain in a united atomistic model (model I) and three standard CG models (model II): the bead center is placed at the geometrical center of the phenyl ring (circles), the geometrical center of the double bond on the main chain (triangles), or the mass center of the whole monomer (squares); (b) illustrations of the bond length, bond angle, and planar angle for the CG model (circles) and the potential functions considered in Figure 3. The merits of selecting each of these CG models[44] can also be evaluated through the following independence check: By computing the following integrand, which evaluates the statistical correlation of adjacent bond angles, for a MEH-PPV oligomer consisting of four monomers

$$I=\sqrt{\int_0^{180}\int_0^{180}[P_{1,2}(\theta_1,\theta_2)-P_1(\theta_1)P_2(\theta_2)]^2\sin\theta_1\sin\theta_2\,\mathrm{d}\theta_1\,\mathrm{d}\theta_2}$$

one obtains 0.020 ± 0.016 (squares), 0.012 ± 0.009 (triangles), and 0.0076 ± 0.0072 (circles), respectively. In the above expression, $P_{1,2}(\theta_1,\theta_2)$ denotes the joint probability distribution function of two adjacent bond angles, and $P_1(\theta_1)$ and $P_2(\theta_2)$ are the probability distribution functions for the individual bond angles (see also Figure 3b). The error bar in each case was estimated on the basis of an equal number of random numbers, as they were properly selected by a standard rejection-acceptance algorithm to ensure the same distribution as the respective $P(\theta)$. Independence may then be claimed when the value of I is comparable with the associated error bar, as is approximately satisfied in all three cases.

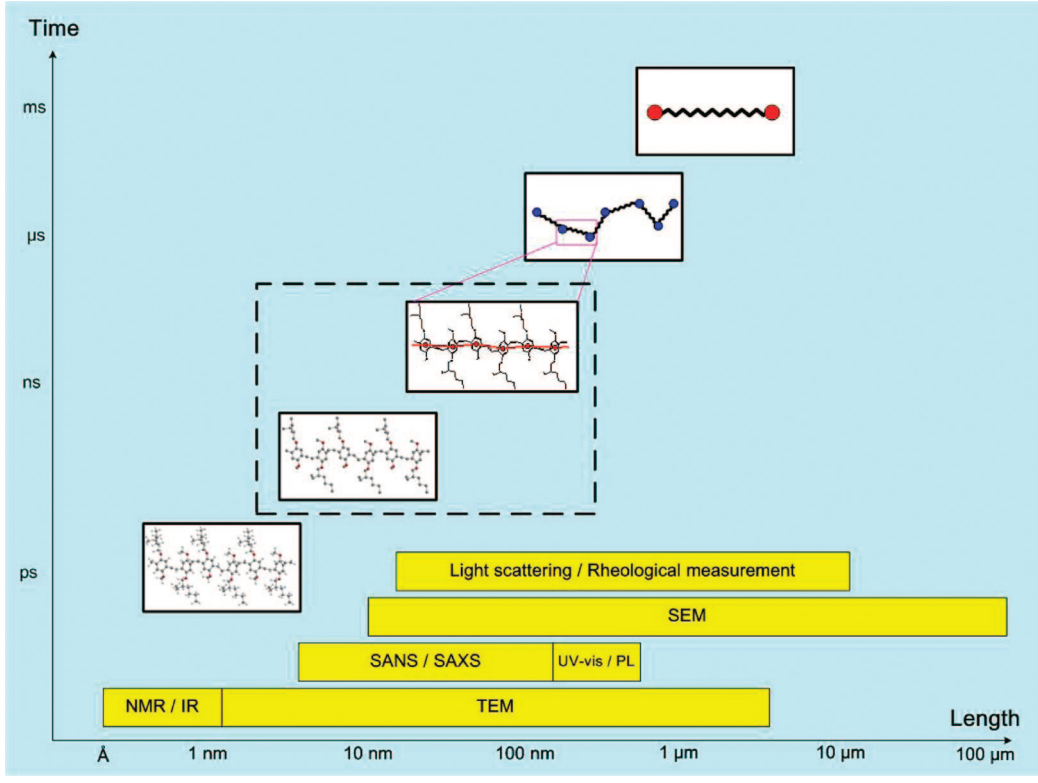

Figure 2. Illustration of the basic ideas of multiscale simulations for MEH-PPV systems. The marked portion is the subject of this CG simulation, while simulation results on other regimes have been reported in early studies.[11−15]

of simulating real large-scale material properties such as aggregation properties. This is especially so for the case of a solution system, for which the cost of simulating the generally uninteresting solvent molecules could be prohibitively high. For this reason, some earlier CG simulations[18,19,26] have taken the advantage of using Langevin dynamics schemes for simulating

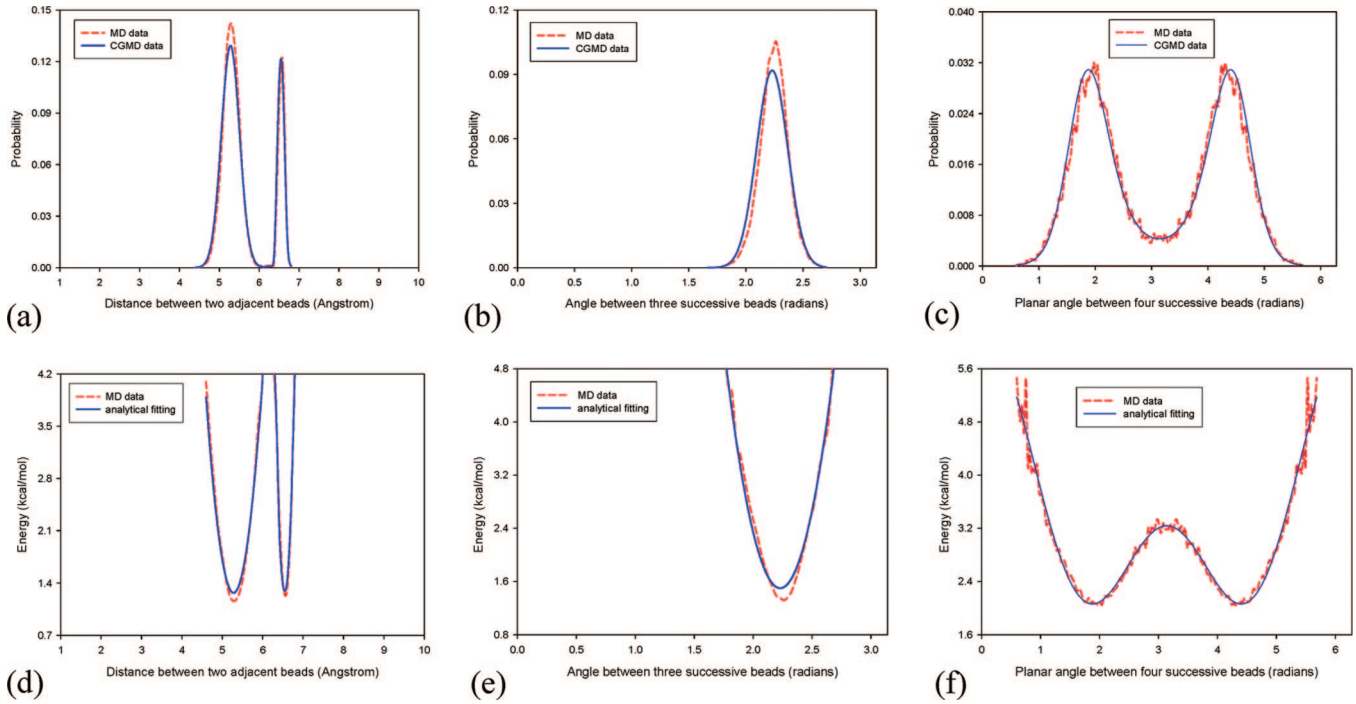

Figure 3. Probability distributions for (a) the bond length, (b) the bond angle, and (c) the planar angle for a MEH-PPV species at 298 K and 1 atm. The Boltzmann-inverted intramolecular potentials are given for (d) the bond length, (e) the bond angle, and (f) the planar angle.

polymer solution systems. We note, however, that the construction of the fluctuation−dissipation forces arising from the coarse-graining of the solvent molecules into a mean-field thermal bath typically required the use of an adjustable parameter (mostly, the frictional drag coefficient) whose connection with its mother atomistic model simulation is unclear. Thus, it is unclear whether the Langevin dynamics utilized is able to properly account for a known solvent quality and its essential impact.

In this work, we propose a CG model and a self-consistent (without using freely adjustable parameters) Langevin dynamics scheme that allow one to capture the structural and the dynamic properties of a polymer solution in a substantially more efficient way than usual MD simulations of a CG model. Consequently, universal single-chain properties that are otherwise difficult to obtain using usual CG simulations may be studied; in addition, access is also allowed for the associated supramolecular aggregation properties. Although the proposed scheme is believed to be applicable to a wider variety of polymer solution systems, we here focus on the application for MEH-PPV solutions. We show that, for the first time, the exact solvent qualities of the investigated solution systems can be evaluated from the simulation. In addition, preliminary simulation results on the supramolecular aggregation properties are obtained and utilized to interpret the general observations from a wide range of recent experimental characterizations.

This article is organized in the following way: In section 2, we summarize the essential chemical and physical features of the MEH-PPV molecule as well as its phenomenological aggregation properties in solution. In section 3, we discuss the construction of a plausible CG model and a self-consistent Langevin dynamics scheme for simulating MEH-PPV in two distinct solvent systems (i.e., aromatic or aliphatic). In section 4, simulation results on both single-chain and supramolecular aggregation properties are presented and discussed. Finally, some concluding remarks are given in section 5.

2. General Background

Conjugated polymers, such as MEH-PPV (see sketch in Figure 1) and other PPV series, bear an essential feature of having alternate double-bond conjugation along the chain backbone and, hence, possess a unique opportunity of serving as polymer-based semiconducting materials.[1,3] The double-bond conjugation, on the other hand, makes the polymer chain relatively stiff and, hence, is difficult to dissolve in most aqueous or organic solvents. Even with some chemical modifications, such as adding side chains to the main polymer backbone, or physical treatments, such as heating or dilution, it appears that polymer aggregation is inevitable in precursor solution. It has now been well perceived that the intra- and interchain aggregations may considerably modify the light-emitting behavior of the solution or the fabricated film due to a modification on the effective conjugation length or through the mechanism of interchain energy transfer.[1,3−9] In addition, the experimentally observed nanostructure for the microdroplets produced by ultradilute MEH-PPV solutions exhibited a close correlation with the solution-phase chain conformation.[13] Therefore, it is of scientific and technological importance to understand the single-chain and aggregation properties in solution, so as to achieve a better control over the material properties in the subsequently dried film through the so-called memory effect.[4]

The most typical way to control the material properties in solution is to make use of different solvents. For the case of a MEH-PPV monomer, which consists of an aromatic backbone and two alkoxy side chains, it is clear that different parts of the molecule bear quite distinct affinities to specific types of solvents. It is, therefore, of interest to understand how the resultant single-chain and aggregation properties would be affected by the use of a particular type of solvent. In experiment, the material properties of conjugated polymer solutions or films were typically studied on the basis of spectroscopic analyses, such as UV−vis adsorption and PL. Although such analyses are sensitive enough to local molecular properties, the detailed

single-chain or aggregation state underlying the spectroscopic features of the solution is difficult to know in general. Other experimental protocols which probe the material properties at larger scales, such as viscometric or light-scattering characterizations, suffer from similar restrictions in resolving the detailed structural features.

Current attempts to understand the molecular properties of MEH-PPV may grossly be depicted in Figure 2, where early simulations and experimental characterizations are classified according to the relevant length/time scales probed. In particular, the marked portion represents the molecular scales aimed to be captured in this simulation. It can be seen that the material properties studied here are of interest in a wide variety of experimental characterizations on semiconducting polymers, including SANS/SAXS measurements, UV−vis/PL characterizations and dynamic/static light scatterings, and are largely beyond the scope of early simulations of MEH-PPV molecules.[11−15] Next, we introduce the essential steps for constructing a plausible CG model and a self-consistent Langevin dynamics scheme for MEH-PPV solutions.

Two different representations of a MEH-PPV oligomer are shown in Figure 1. Model I resembles the usual atomistic model, except that all hydrogen atoms have been lumped into their mother carbon atoms. Model II presents three potential candidates for the present CG model, by treating each repeating unit (or monomer) as one particle or "bead". In principle, selection among these CG models is to achieve the best compromise between capturing the essential molecular details and computational convenience.[17] It came to our notice, however, that the presence of a large dangling side-chain group in the MEH-PPV monomer makes the CG model adopting the mass center of the whole monomer (i.e., filled squares) an inadequate choice. The reason is that the relatively free positioning fluctuations of the large side-chain group result in an apparent mobility of the CG particle, and consequently lead to spurious flexibilities in the CG bond length and angles (in this case, the predicted persistence length was noted to be about half of that based on the other two CG models). This observation, in fact, poses an important general consideration in the CG simulation of a polymer chain with large side-chain groups. On the other hand, the predicted single-chain properties, including persistence length and radius of gyration, based on the other two CG models are in excellent agreement, and the one which centers the CG bead at the geometrical center of the phenyl ring (i.e., filled circles) is adopted for its better consistency with the later modeling of intermolecular potential.

Possessing a pair of asymmetric alkoxy side chains and an aromatic backbone has made MEH-PPV an amphiphilic polymer, leading to a rich variety of chain conformations and supramolecular aggregations in solution. For some special applications, such as mixing aliphatic/aromatic solvent systems, it might be necessary to treat the two side chains as independent beads in the CG model. Besides, the planar phenyl ring of each MEH-PPV monomer provides the essential local $\pi-\pi$ interactions often believed to be an important source of polymer aggregation. Although the aforementioned features could be among the important considerations in constructing a CG model for MEH-PPV, we here adopt a more standard CG model with the beads placed at the geometrical center of the phenyl rings (i.e., filled circles of Figure 1a, model II). For a MEH-PPV chain as long as presently studied (i.e., $M_n \approx 80\,000$ Da or 300 monomers per chain), $\pi-\pi$ interactions that are necessary for a more precise account of the local structural feature might further be coarse-grained in computing large-scale material properties that are of primary interest in this study. On the other hand, typical synthesized defects, such as the cis and tetrahedral defects, make the planar and rodlike structure associated with an ideal, all-trans MEH-PPV practically inaccessible, leading to a rich variety of chain conformations in various solvents. Since the actual amount and distribution of these defects are difficult to know in practice, this study focuses on model MEH-PPV chains with an alternating cis−trans conformation (see sketches in Figure 1b). While conserving a fully conjugated configuration, the cis conformation was noticed to result in a slight tilting of two adjacent phenyl rings as the favorable equilibrium state, thus breaking up the planar feature of ideal MEH-PPV molecules.[12] The resultant chain conformation thereby allows for a systematical exploration of the collapsed chain conformation under varying solvent quality.[13,14] As we shall show, the persistence lengths so obtained are in close agreement with recent experimental estimations, suggesting that the impact of synthesized defects is reasonably captured. In general, it will be demonstrated that the present CG model is capable of capturing essential material properties of MEH-PPV in two representative solvent systems as implied by recent experimental observations and simulation results. Investigation based on a different CG model for mixed solvent systems is left to a future work. In what follows, we describe how the simulation results based on model I may be utilized to reconstruct the force fields and the Langevin dynamics for the CG model chosen for model II (circles), which will be employed to compute all the single-chain and aggregation properties presented in this work.

3. Model Construction and Simulation Protocol

The MD simulation of model I was carried out using usual Newton's equations of motion. The calculations were performed in a supercomputer with four CPUs running in parallel; an existing software package DLPOLY2[32] and incorporated force fields[33] were used. The simulation results were mainly utilized to provide essential statistical trajectories for the bond length and angles as redefined in the CG model (i.e., model II). To ensure that the data collected for model I well represent the equilibrium distributions for local bond length and angles, the initial chain conformations for model I were created and subsequently equilibrated with the aid of a Monte Carlo scheme. The computed statistical trajectories, after the Jacobian correction,[20,24] for the bond length and two bond angles, respectively, are shown in Figure 3 along with their Boltzmann-inverted potentials:

$$U(z) = -k_B T \ln P(z) \tag{1}$$

where $k_B T$ is the Boltzmann constant times the absolute temperature, and $P(z)$ is the probability distribution function of the variable z (i.e., bond length or angle) defined in the CG model. A fundamental requirement that must be fulfilled here is that any variable chosen for z must be independent variable[17,20,24] (see also the footnotes of Figure 1). Parts a−c of Figure 3 compare the predictions of the CG model with those of model I; parts d−f of Figure 3 show the analytical fitting of the inverted potential functions that were later employed by the CG model, with the parameters determined by using an automatic simplex optimization. Excellent agreement has been achieved between atomistic MD and CG simulation data, which should guarantee that the chain conformation and associated structural and dynamic properties are well captured in subsequent CG simulations. The functional forms, model parameters,

TABLE 1: (a) Specifications of the Simulation System and (b) Potential Functions and Model Parameters[a]

(a) Specifications of the Simulation System

system	no. of chains (no. monomers per chain)	solvent
Figures 5a and 6	MEH-PPV ($n = 300$) × 1	toluene
Figures 5b and 6	MEH-PPV ($n = 300$) × 1	chloroform
Figure 7	MEH-PPV ($n = 100-500$) × 1	toluene or chloroform
Figure 8a	MEH-PPV ($n = 100$) × 6	toluene
Figure 8b	MEH-PPV ($n = 100$) × 6	chloroform
Figure 9a	MEH-PPV ($n = 100$) × 10	toluene
Figure 9b	MEH-PPV ($n = 100$) × 10	chloroform

(b) Potential Functions and Model Parameters

intramolecular interactions (within a constant vertical shift)		notation	parameters
bond length	$U_{bond} = -k_B T \ln[A_1 e^{-[(r-r_{1,0})/B_1]^2} + A_2 e^{-[(r-r_{2,0})/B_2]^2}]$	k_B: Boltzmann constant T: absolute temperature A_1, B_1, A_2, B_2: four fitting constants $r_{1,0}$, $r_{2,0}$: two equilibrium bond lengths	$A_1 = 0.118$ $B_1 = 0.323$ Å $r_{1,0} = 5.280$ Å $A_2 = 0.119$ $B_2 = 0.112$ Å $r_{2,0} = 6.548$ Å
bond angle	$U_{angle} = k_B T[(\theta - \theta_0)/B]^2$	B: fitting constant θ_0: equilibrium bond angle	$B = 0.193$ rad $\theta_0 = 2.230$ rad
planar angle	$U_{plan} = (V_1/2)[1 + \cos(\phi)] + (V_2/2)[1 + \cos(2\phi)]$	V_1, V_2: two fitting constants	$V_1 = 2.958$ kcal/mol $V_2 = 2.428$ kcal/mol
intermolecular interactions		**notation**	**parameters**
van der Waals	$U_{vdw} = 4\varepsilon_{ij}[(\sigma_{ij}/r_{ij})^{12} - (\sigma_{ij}/r_{ij})^6]$	ε_{ij}, σ_{ij}: van der Waals parameters	$\varepsilon_{TT} = 0.323$ kcal/mol $\sigma_{TT} = 5.550$ Å $\varepsilon_{CC} = 0.292$ kcal/mol $\sigma_{CC} = 4.920$ Å $\varepsilon_{MM} = 0.120$ kcal/mol $\sigma_{MM} = 5.730$ Å

[a] Other pair interaction parameters were estimated by $\varepsilon_{ij} = (\varepsilon_{ii} \times \varepsilon_{jj})^{1/2}$ and $\sigma_{ij} = {}^1/_2(\sigma_{ii} + \sigma_{jj})$, where T, C, and M indicate toluene, chloroform, and MEH-PPV monomer, respectively.

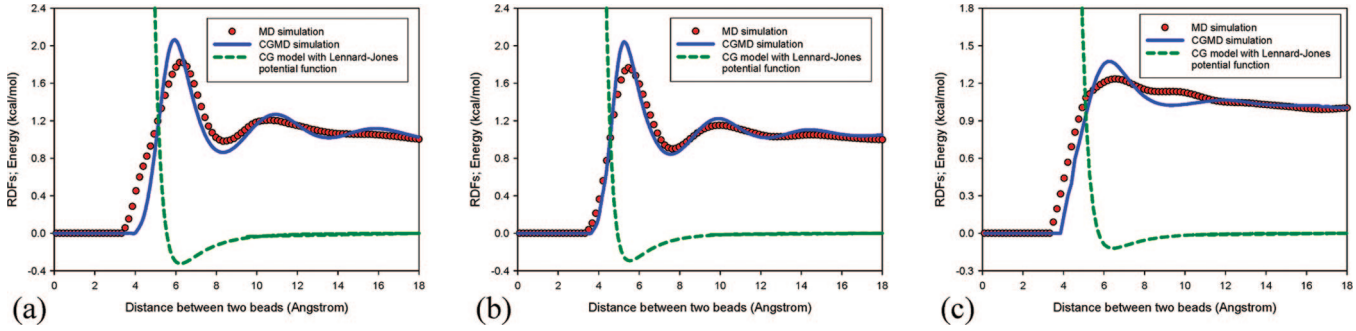

Figure 4. Radial distribution functions (RDFs) and potential energy functions at 298 K and 1 atm for the baths of (a) toluene, (b) chloroform, and (c) MEH-PPV monomer.

and detailed specifications of the simulation system are compiled in Table 1.

Similarly, the intermolecular potential for nonbonded beads in the CG model may be constructed using the radial distribution function (RDF) obtained for model I:

$$G(r) = \frac{n(r)}{\rho 4\pi r^2 \Delta r} \tag{2}$$

where $n(r)$ is the mean number of particles lying within the shell defined by the radial distances r and $r + \Delta r$, respectively, and ρ is the bulk number density. In this case, the solvent molecules are modeled as single particles, as is the case with the polymer monomer. Note, however, that since the RDF so obtained is strictly a consequence of many-body interactions, the corresponding Boltzmann inversion does not necessarily yield the real pair interactions, unless the system remains sufficiently dilute and noninteracting. Using the inverted function as a first guess, an iterative procedure can nevertheless be adopted to find an effective pair interaction potential that best describes the RDF given.[17,24] Thus, optimal Lennard-Jones potential functions (see a detailed specification of model parameters in Table 1) were chosen to mimic nonbonded potentials for the CG model. Comparisons of the predicted RDFs from two different simulations are provided in Figure 4.

To this end, usual MD simulations of the CG model have been carried out to provide the comparisons shown above. For most of the subsequent analyses, however, we consider a different approach which bears an obvious advantage of being substantially more efficient. The simulation is then shown to be able to capture both the dynamic and the structural properties as might be obtained from the corresponding, more expensive MD simulation. The central idea is that a self-consistent

Langevin dynamics of the CG model is constructed using the predictions of the atomistic model for single-particle diffusivities. As an important consequence, much longer MEH-PPV chains ($M_n \approx 80\,000$ Da) and their supramolecular aggregates as well as real times (up to several hundred nanoseconds) can be simulated in a single-CPU personal computer. Simulation results so obtained have interesting implications for understanding the solution properties of MEH-PPV, as we discuss later.

We begin with the Langevin equation of motion for a usual Brownian particle without hydrodynamic interactions:

$$m_i \frac{d^2\mathbf{r}_i}{dt^2} = -\varsigma_i \frac{d\mathbf{r}_i}{dt} + \sum_j \mathbf{F}_{ij} + \xi_i \tag{3}$$

where m_i and r_i are the mass and positional vector of the ith bead on a certain polymer chain, respectively, $\sum_j F_{ij}$ and ξ_i are the sum of the conservative forces (i.e., the intra- and intermolecular forces) and the random force, respectively, acting on the same bead, and ς_i (sometimes defined as $m_i\varsigma_i$)[34] is the frictional drag coefficient. Because the relationship between the random Brownian force and the mean-field frictional drag coefficient must be dictated by the fluctuation−dissipation theorem, generally given in form of the Einstein relation, $\varsigma_i = k_BT/D_i$, it is possible to estimate the frictional drag coefficient, ς_i, using the predicted particle diffusivity, D_i, from the atomistic MD simulation for a given solvent. Then, the following expression of Brownian forces with a Gaussian statistics can be constructed:

$$\langle \xi_i \rangle = 0 \quad \text{and} \quad \langle \xi_i(t)\xi_j(t) \rangle = 2\varsigma_i k_B T \delta_{ij} \mathbf{I} \tag{4}$$

In eq 4, the broken brackets denote taking the ensemble average of the quantity within them, I is a unit tensor, and δ_{ij} is the Kronecker delta function.

Several things must be noted here. First, although the polymer particle described in this CG model might not be treated as a usual Brownian particle, whose mass should be sufficiently larger than those of surrounding solvent particles, it will be shown that the Einstein relation and the Brownian forces so constructed seem to lead to results in good agreement with what directly obtained from the MD simulation of the CG model. On the other hand, the commonly employed extension—the Einstein-Stokes law—which involves using the bulk solvent viscosity to estimate the particle diffusivities, fails evidently in the current level of coarse-graining, as might be expected. Note also that it has not been uncommon using similar Langevin dynamic equations to simulate polymer solution or melt systems at a similar level of coarse-graining.[18,19,26] The major difference is that the frictional drag coefficient has typically been treated as adjustable and, hence, lacks a definite link with the prediction of the atomistic model. In summary, it appears that the Einstein relation remains applicable even for a CG particle as small as a polymer monomer. By contrast, the subsequent extension—the Einstein-Stokes law—is subject to the restriction of continuum mechanics. This issue will be revisited in the next section, as the simulation results of the center-of-mass chain diffusivities are examined against the previous law.

From the MD simulation of model I, the diffusivities of MEH-PPV monomer in toluene and in chloroform have been estimated to be $D_{MT} = 2.83 \times 10^{-9}$ and $D_{MC} = 7.47 \times 10^{-9}$ m^2/s, respectively, at $T = 298$ K and 1 atm. Accordingly, one obtains $\varsigma_{MT} = k_BT/D_{MT} = 1.45 \times 10^{-12}$ kg/s and $\varsigma_{MC} = k_BT/D_{MC} = 0.55 \times 10^{-12}$ kg/s as the effective drag coefficients, respectively. To this end, the Langevin dynamics of a MEH-PPV chain may be tracked by using eqs 3 and 4 along with the intra- and intermolecular potentials obtained earlier.

TABLE 2: Comparisons between the Langevin Dynamics Simulation (CGLD) and the Molecular Dynamics Simulation (CGMD) of Model II (Circles) for the Predicted Radius of Gyration and Center-of-Mass Diffusivity, Respectively[a]

100 monomer per chain	radius gyration (Å)	diffusivity (m^2/s)
CGMD	$R_{g,MT} = 26.77 \pm 1.42$	$D_{MT} = 2.97 \times 10^{-10}$
CGLD	$R_{g,MT} = 26.48 \pm 1.02$	$D_{MT} = 2.62 \times 10^{-10}$
CGMD	$R_{g,MC} = 33.40 \pm 1.19$	$D_{MC} = 5.90 \times 10^{-10}$
CGLD	$R_{g,MC} = 34.03 \pm 0.97$	$D_{MC} = 4.66 \times 10^{-10}$

[a] These two simulations utilized the same intra- and intermolecular force fields at $T = 298.15$ K and 1 atm, and the total simulation time is 1.6 ns for both cases. The CGMD simulation was carried out in a parallel computation system (IBM-P690 with 4 CPUs) using the software DLPOLY2, and the total computation time was ca. 36 h. The CGLD simulation was performed in a single-CPU personal computer using eqs 3 and 4, and the total computation time was ca. 10 min.

Table 2 compares the predicted single-chain diffusivity and radius of gyration, respectively, for the CG model using two different simulation methodologies. It is readily evident that the Langevin dynamics simulation is capable of capturing the results of the MD simulation on both the dynamic and the structural properties of a single MEH-PPV chain in two different solvent systems. Moreover, for the results shown in Table 2, it takes ca. 36 h of the MD simulation with four CPUs running in parallel, while it requires only about ten minutes for the Langevin dynamics simulation executed in a single-CPU personal computer. In fact, only through the Langevin dynamics simulation will it be possible for us to investigate polymer chain lengths close to what typically studied in real experiment, and, in particular, to gain some insight into the properties of supramolecular aggregates formed by several MEH-PPV chains of comparable length.

In simulating eq 3, the Velocity Verlet algorithm[34] was used with a time step of 8 fs (see a later discussion). As is usually done, periodic boundary conditions were applied in all three spatial directions. Initially, a Monte Carlo scheme[34,35] was used to create independent MEH-PPV chains with minimum configuration energies. Each chain was further equilibrated for a number of steps ca. 3×10^5, which warrants equilibrations of local bond length and angles and facilitates a fast equilibration in the overall chain configuration in subsequent MD simulations. For the results reported in the next section, the simulated MEH-PPV chain typically consists of 300 monomers per chain (or $M_n \approx 80\,000$ Da), which falls in the regime of the sample molecular weights as typically investigated in experiments.[9,11]

Before closing the introduction of the simulation protocol, we would like to add a few remarks. In the spirit of the proposed Langevin dynamics scheme, the effect of solvent quality might be regarded as being self-consistently accounted for via the balance between the fluctuation−dissipation forces (i.e., the frictional drag force and the Brownian force) and the conservative forces (i.e., the intra- and intermolecular forces). This is, in fact, an interesting feature in the present simulation of a polymer solution, and is to be contrasted with typical Langevin dynamics simulations in which a specific solvent quality was mimicked by independently adjusting the parameters of intermolecular forces.[18,19,36,37] On the other hand, the effect of hydrodynamic interactions, which are omitted in this work yet are expected to have certain influences on the dynamic and even structural properties, remains to be explored in a future study. Generally speaking, this specific effect might be essential for a precise setting of the real time of the simulation,[18] as well as

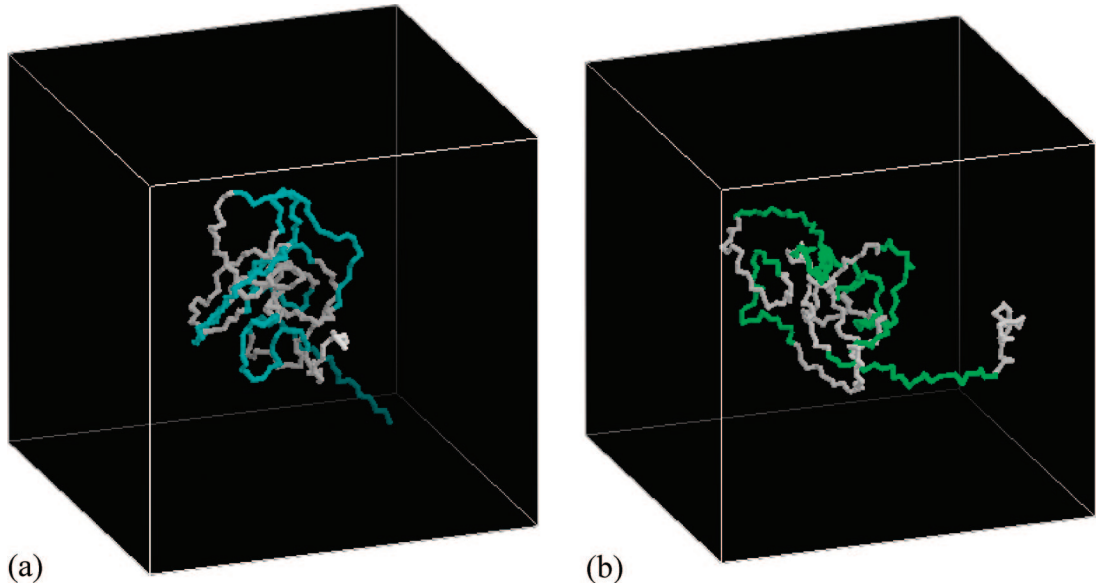

Figure 5. Realization of a single MEH-PPV chain in (a) toluene or (b) chloroform. The simulation is carried out at $T = 298$ K and 1 atm for a simulation time 8 ns, with the same initial chain conformation obtained from a Monte Carlo simulation.

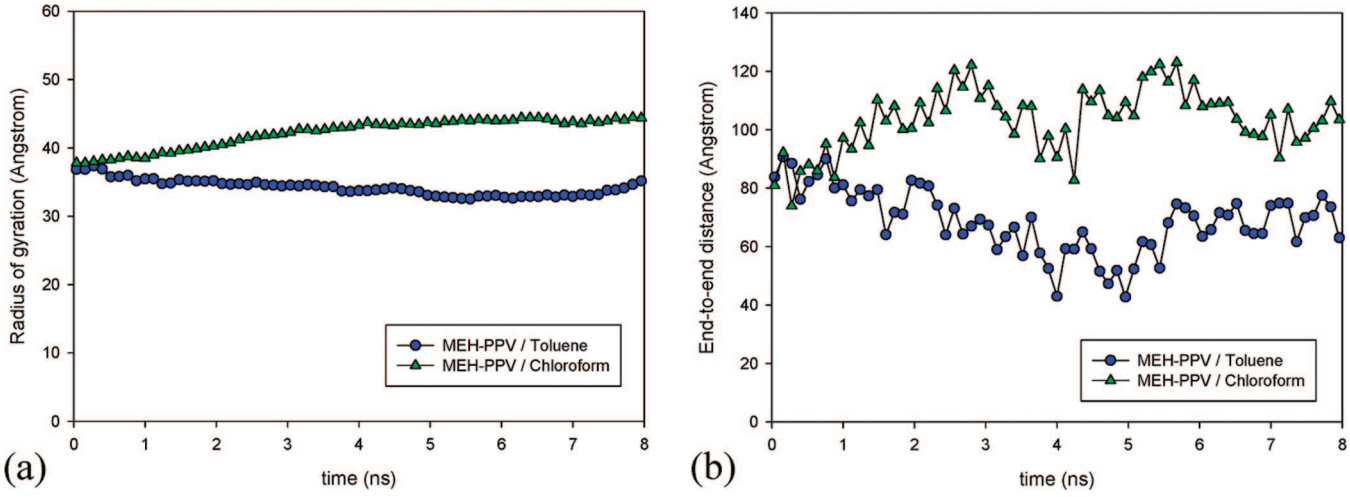

Figure 6. (a) Predicted radii of gyration and (b) end-to-end distances of a MEH-PPV chain in two different solvent systems as functions of time.

for accounting for some fundamental dynamic properties of polymer chains in dilute solution.[38,39]

4. Results and Discussion

4.1. Single-Chain Properties. As has been noted earlier, the single-chain properties of MEH-PPV in solution are difficult to obtain in real experiment due to a strong tendency for the chain to form aggregates in essentially all solvents known. Computer simulations are, therefore, valuable in providing access to the single-chain behavior in solution; the effect of solvent quality on the aggregation properties may also be explored systematically.

Figure 5 shows representative realization of a single MEH-PPV chain in chloroform or in toluene. The chain conformation seen here is essentially the result of the competition between chain stiffness and intermolecular interactions under a poor-solvent condition. Apparently, the solvent quality has a very pronounced effect on MEH-PPV chain conformation. Considering the effect of chemical affinity, the MEH-PPV chain was earlier believed to assume a more extended chain conformation in an aromatic solvent, such as toluene, due to its superior affinity to the chain backbone.[4,5] And the chain was expected to be more coil-like in an aliphatic solvent, such as chloroform, which prevents the exposure of chain backbone to the solvent. Clearly, these conjectures are at odds with the present CG simulation, which suggests that the overall solvent quality (to be discussed below), but not the local chemical affinity, determines the ultimate chain conformation. The present results are, in fact, consistent with early MD simulations.[11,14]

For a polymer chain with chemical amphiphicility like MEH-PPV, the apparent solvent quality is a curious quantity to explore. Namely, selective affinities of a particular type of solvent to different parts of the MEH-PPV chain make the resultant solvent quality somewhat unpredictable. In an atomistic MD or CG simulation, solvent quality can, in principle, be evaluated by examining the scaling behavior of the mean coil size with respect to the degree of polymerization. In practice, however, this procedure could pose a serious challenge to most atomistic MD and even CG simulations, had the simulation of solvent particles not properly tackled. With the aid of the Monte Carlo scheme mentioned earlier and, in particular, the proposed Langevin dynamics scheme, the chain behavior near equilibrium

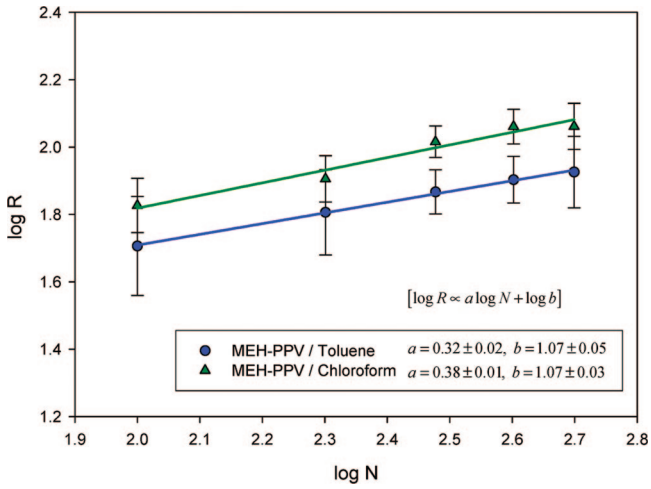

Figure 7. Scaling relationships for the mean end-to-end distance (R) as functions of molecular weight (N denotes the number of monomers per chain) for single MEH-PPV chain in two different solvent systems.

becomes accessible in this simulation. Figure 6 shows the predicted radius of gyration and end-to-end distance, respectively, for single MEH-PPV chains in toluene or in chloroform. In general, one sees that the coil size of MEH-PPV is larger in chloroform than in toluene (i.e., $R_{g,MC} = 43.7 \pm 0.5$ Å and $R_{g,MT} = 34.4 \pm 0.7$ Å). The observed effects of solvent were in qualitative agreement with an early experimental result based on fluorescence correlation spectroscopy.[13] In particular, the scaling exponents (0.32 ± 0.02 in toluene and 0.38 ± 0.01 in chloroform at $T = 298$ K) retrieved from the plots shown in Figure 7 clearly indicate that both solution systems fall well below the so-called Θ-condition (which bears a theoretical exponent 0.5), yet chloroform has a better solvent quality than toluene. To the best of our knowledge, this is the first time that the exact solvent qualities for MEH-PPV solutions at a given temperature have been reported in terms of fundamental scaling laws for the coil size. In fact, a better solvent quality found for the chloroform system is in agreement with the common experience that MEH-PPV dissolves more readily in chloroform than in toluene. On the other hand, spectroscopic observations generally indicated that the adsorption or light emission curves of MEH-PPV solutions were more red-shifted when an aromatic solvent was used.[4] Recent SANS observations also suggested that MEH-PPV bears a higher degree of aggregation in toluene than in chloroform.[10] Both phenomena imply that the aggregation properties of MEH-PPV solutions are closely correlated with the solvent qualities here explored, as we comment later.

Another fundamental chain property that is usually of interest is the persistence or Kuhn length, which yields information about the stiffness of a polymer chain. The persistence length, denoted as L_P, of a homopolymer is estimated using the following relation:[40]

$$L_p = \sum_{k \geq j} \left\langle \frac{\mathbf{Q}_j \cdot \mathbf{Q}_k}{a} \right\rangle \quad (5)$$

where Q and a are the bond vector and bond length, respectively, and the indices j, k sum over all segments of the same chain. We noticed, however, that persistence length has customarily been estimated using a formula which essentially utilizes the chain contour length to replace the Kuhn chain length.[12,41] Such a treatment will result in a somewhat smaller persistence length. Currently, the persistence length of MEH-PPV is estimated to be 65.1 ± 11.8 Å in toluene and 73.3 ± 12.5 Å in chloroform, which correspond to the mean end-to-end distance of about 25 MEH-PPV monomers (or, equivalently, there are 50 MEH-PPV monomers in a Kuhn segment). These results are in close agreement with light scattering data, ca. 60 Å in *p*-xylene,[41] and a recent SANS estimation, ca. 87.5 Å in chloroform.[10] Note that the persistence length might be sensitively affected by the amount and distribution of the synthesized defects.[12] In contrast, our observations suggested that the solvent qualities determined earlier are relatively insensitive to the detailed chain conformation. The reason could be that the solvent-quality dependence of the coil size is basically controlled by the interactions between the polymer and solvent molecules as long as the chain length stays sufficiently large with respect to the Kuhn length. For comparison, we mention that early MD simulation[42] and SANS measurement[43] have yielded the persistence lengths for two typical flexible polymers, i.e., polyethylene (PE) and polystyrene (PS), as 4.7 and 9.2 Å, respectively. The semiflexible feature of the MEH-PPV molecule is thus evident.

In addition to the structural features discussed above, knowledge of the dynamic properties of single MEH-PPV chains in solution helps understand the aggregation property.[11] For a similar reason, the dynamic properties of single MEH-PPV chains are difficult to retrieve from real experiments because of the problem of chain aggregation. From the time-dependent mean-square chain displacement at long times, the center-of-mass diffusivities of MEH-PPV were estimated to be $D_{G,MT} = 7.51 \times 10^{-11}$ m^2/s and $D_{G,MC} = 9.62 \times 10^{-11}$ m^2/s, respectively. Note that determination of a dynamic quantity in a CG simulation would require a known relationship between the CG time scale and that in the atomistic simulation. There are, in principle, several ways to gain such information.[24] Here, the unknown time shift has been determined by fitting the CG simulation data with the atomistic simulation data on the autocorrelation function of the end-to-end vector of a MEH-PPV oligomer (i.e., with 6 monomer units).

Comparing these results of chain diffusivity with those obtained earlier for the monomer diffusivity, i.e., $D_{MT} = 2.83 \times 10^{-9}$ m^2/s and $D_{MC} = 7.47 \times 10^{-9}$ m^2/s, one sees that the disparity in the monomer mobility smears off in the corresponding full-chain diffusivity. The significance of this phenomenon is 2-fold. First, it indicates how the dynamic behavior of a small molecule or oligomer would, in general, be governed by the chemical affinity or intermolecular interactions with the solvent molecules. With increasing chain length, however, the whole chain behaves like a macromolecule, whose dynamic properties are primarily dictated by the mean-field drag or the solvent viscosity. Given that the viscosities are nearly identical for the two solvents considered, it might be expected that the center-of-mass chain diffusivities should stay similar, as observed here. On the other hand, the remaining disparity, which conflicts even qualitatively with the prediction of the Einstein-Stokes law, is reminiscent of an effect of solvent quality on single-chain dynamic properties.[39]

4.2. Dynamics and Structures of Supramolecular Aggregation. One of the main objectives of this work is to gain some insight into the supramolecular aggregation properties of MEH-PPV in solution, as well as to understand the impact of solvent quality. As mentioned earlier, various experimental protocols have been utilized to characterize the aggregation properties of MEH-PPV solutions. However, the information obtained was mostly qualitative, and the detailed aggregation structure or the kinetics of its formation was typically unknown. Although practically accessible aggregation features remain

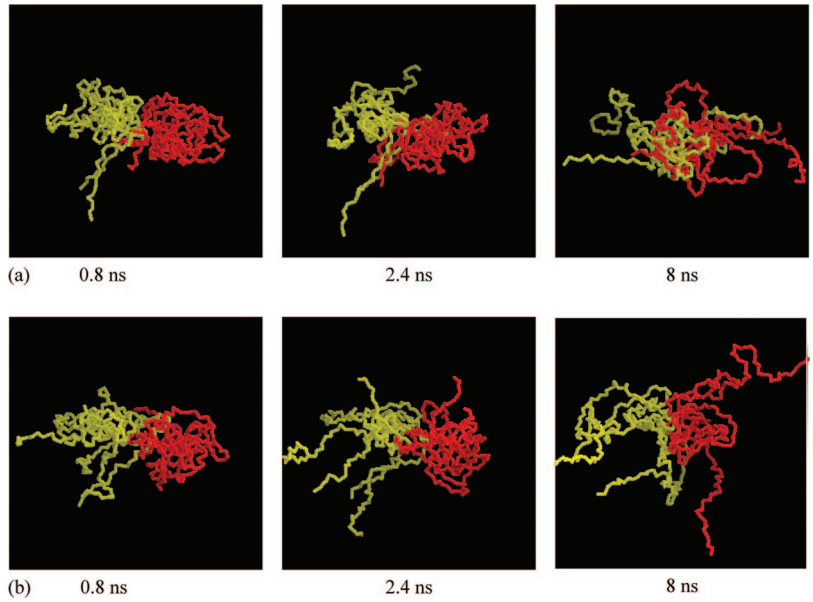

Figure 8. Snapshots of the process of coalescence of two MEH-PPV aggregates in (a) toluene or (b) chloroform at various times at $T = 298$ K and 1 atm.

extremely limited in this simulation, some preliminary observations discussed below seem to shed light on the general observations from a wide range of recent experiments. Note, however, that substantially more localized aggregation properties, as might be studied using first-principles calculations, that are directly responsible for the spectroscopic features[14] of the solution are beyond the scope of this work.

Figure 8 demonstrates the process of coalescence of two small aggregate clusters, each consisting of three MEH-PPV chains. The resultant aggregate cluster is considerably looser in chloroform than in toluene, with the radii of gyration of the clusters being ca. 54.3 and 41.6 Å, respectively, after a time 8 ns. To further characterize the structural compactness of an aggregate cluster, we utilize the following definition of monomer density:

$$\rho_N = \frac{N_b}{\frac{4}{3}\pi {R_g}^3} \tag{6}$$

where N_b and R_g are the number of monomers and radius of gyration of the cluster, respectively. This definition yields $\rho_N = 0.9$ bead/nm^3 in chloroform and $\rho_N = 2.0$ bead/nm^3 in toluene; the disparity in the compactness of the aggregation structure is thus evident. It can also be seen that the MHE-PPV chains form loosely entangled network in chloroform, as contrasted with a deeper nucleation observed in toluene. Figure 9 demonstrates how initially separated chains later collapse into a single aggregate cluster. The resultant aggregation structures, $R_g = 86.8$ Å and $\rho_N = 0.4$ bead/nm^3 in chloroform and $R_g = 70.4$ Å and $\rho_N = 0.7$ bead/nm^3 in toluene bear a similar contrast as noted earlier in Figure 8. Below, we remark on some interesting implications that seem to be reached from the simulation results already presented.

Solvent quality has, in general, been defined according to known single-chain properties, such as what has been discussed earlier. This fundamental solution property yields information of the relative coil size in a specific solvent and at a given system temperature. It, however, generally does not imply the associated aggregation property under a poor-solvent condition. Given that the predicted aggregation features of MEH-PPV solutions seem to be in good agreement with early experimental observations,[4,5,9−11] one is led to the conclusion that the ways in which solvent quality affects the single-chain and aggregation properties, respectively, are basically no different. In other words, the basic structural features in solution are virtually governed by the same solvent quality as retrieved from a plot like Figure 7.

Finally, we remark on possible future applications of the proposed CG model and simulation scheme. First, the monomer densities reported here may be utilized to achieve a rough estimation of the average number of MEH-PPV chains in an aggregate cluster, whose size can readily be inferred from dynamic or static light scattering measurements. Second, for a direct comparison with SANS/SAXS data, it might be possible to compute the scattering structural factors using proper ensemble averages of the single-chain and supramolecular aggregation realizations obtained from a similar CG simulation. Third, the proposed model and simulation may serve as a basis for the construction of further coarse-grained models and simulations, so that larger-scale material properties can be investigated. Finally, the model construction and simulation protocol proposed in this work should be applicable for a wider variety of polymer solution systems. In summary, through a self-consistent hierarchy of coarse-graining procedures, such as what has been demonstrated in this work as well as in an earlier Brownian dynamics simulation[15] for the case of MEH-PPV solutions, it is possible to gain comprehensive molecular insights of a polymer solution system that, in turn, are essential to interpret results from a wide range of experimental characterizations. This is, in fact, among the important goals of performing multiscale simulations for systems with complex supramolecular structures and physical interactions.

5. Conclusion

We have proposed a CG model and Langevin dynamics scheme to investigate the single-chain and supramolecular aggregation properties in solution of a model semiconducting conjugated polymer (i.e., MEH-PPV with an alternating cis−trans conformation). An important feature of the proposed CG scheme is that the fluctuation−dissipation forces arising from the use of a solvent field were self-consistently constructed, without

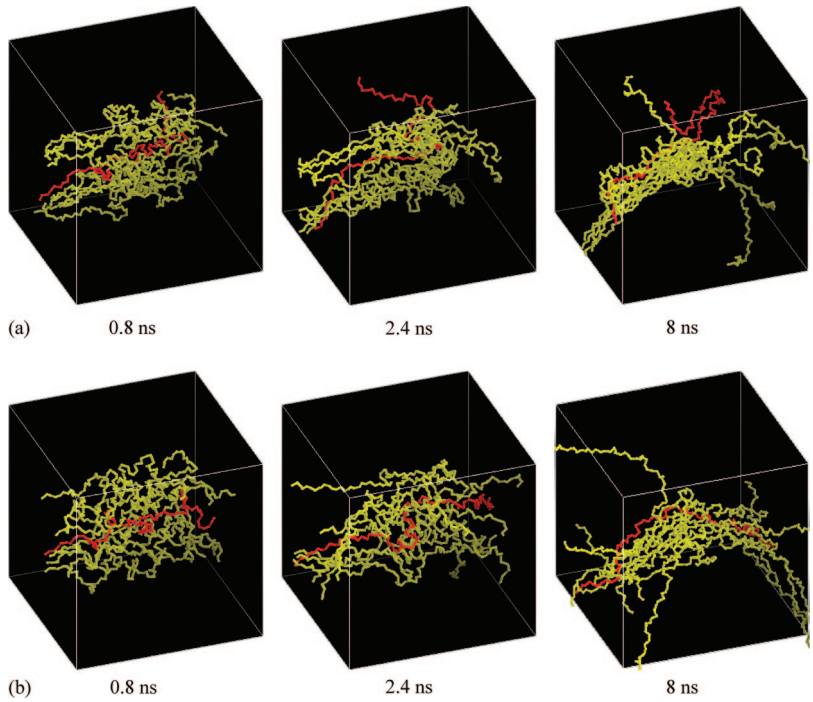

Figure 9. Snapshots of 10 MEH-PPV chains collapsing into an aggregate cluster in (a) toluene or (b) chloroform at various times at $T = 298$ K and 1 atm, where all chains were initially placed in parallel and assumed a fully extended chain configuration.

using freely adjustable parameters, from the measured monomer diffusivity in a given solvent through the atomistic MD simulation. Besides, it was noticed that the presence of a large dangling side-chain group of MEH-PPV requires a special consideration in selecting a plausible CG particle. It was demonstrated that the effect of solvent quality on the structural features can well be captured, and the chain dynamics was also naturally retained. As an important consequence, it became possible to investigate single-chain and supramolecular aggregation properties that were otherwise inaccessible by usual CG simulations or real experiments.

Chemical amphiphicility and the hairy-rod feature have made MEH-PPV an interesting polymer for studying, with strong practical motivations, the solvent dependences of the single-chain and supramolecular aggregation structures in solution. Thus, two distinct solvent systems (i.e., aromatic or aliphatic) have been examined using the proposed CG simulation, and the major achievements were as follows: The simulation on single-chain properties yielded, for the first time, the scaling exponents (i.e., 0.32 in toluene and 0.38 in chloroform at $T = 298$ K) characterizing the exact solvent qualities, confirming a generally poor solvent quality for MEH-PPV solutions. The relative coil size was a clear indication of the overall solvent quality of a particular solution system. Specifically, it was found that an aliphatic solvent—chloroform, which is relatively attractive to the side-chain (but not to the backbone) units of MEH-PPV, turned out to result in an overall better solvent quality and, hence, a larger coil size in solution. Moreover, the persistence lengths for both solvent systems were estimated to be $L_p \approx 70$ Å (which corresponds to about the mean end-to-end distance of 25 MEH-PPV monomers), in close agreement with recent neutron/light scattering data. On the other hand, preliminary observations on supramolecular aggregation properties suggested that the aggregation structure is considerably more compact in toluene—a poorer solvent, despite its superior affinity to the MEH-PPV backbone. This trend was also in agreement with the general observations in recent experiments, suggesting that the solvent quality determined from single-chain data may as well be utilized to infer the associated aggregation properties.

Acknowledgment. The authors appreciate constructive comments of the reviewers. This work is supported by the MOE Program for Promoting Academic Excellence of Universities under the Grant No. 96-2752-E-007-006-PAE. The resource provided by the National Center for High-Performance Computing of the ROC is gratefully acknowledged.

References and Notes

(1) Burroughes, J. H.; Bradley, D. D. C.; Brown, A. R.; Marks, R. N.; Mackay, K.; Friend, R. H.; Burn, P. L.; Holmes, A. B. *Nature* **1990**, *347*, 539.

(2) Kraft, A.; Grimsdale, A. C.; Holmes, A. B. *Angew. Chem., Int. Ed.* **1998**, *37*, 402.

(3) Friend, R. H.; Gymer, R. W.; Holmes, A. B.; Burroughes, J. H.; Mark, R. N.; Taliani, C.; Bradley, D. D. C.; Dos Santos, D. A.; Brédas, J. L.; Löglund, M.; Salaneck, W. R. *Nature* **1999**, *397*, 121.

(4) Nguyen, T. Q.; Doan, V.; Schwartz, B. J. *J. Chem. Phys.* **1999**, *110*, 4068.

(5) Shi, Y.; Liu, J.; Yang, Y. *J. Appl. Phys.* **2000**, *87*, 4254.

(6) Liu, J.; Shi, Y.; Ma, L.; Yang, Y. *J. Appl. Phys.* **2000**, *88*, 605.

(7) Collision, C. J.; Rothberg, L. J.; Treemaneekarn, V.; Li, Y. *Macromolecules* **2001**, *34*, 2346.

(8) Chen, S. H.; Su, S. C.; Huang, Y. F.; Su, C. H.; Peng, G. Y.; Chen, S. A. *Macromolecules* **2002**, *35*, 4229.

(9) Chen, S, H.; Su, A. C.; Chang, C. S.; Chen, H. L.; Ho, D. L.; Tsao, C. S.; Peng, K. Y.; Chen, S. A *Langmuir* **2004**, *20*, 8909.

(10) Ou-Yang, W. C.; Chang, C. S.; Chen, H. L.; Tsao, C. S.; Peng, K. Y.; Chen, S. A.; Han, C. C. *Phys. Rev. E* **2005**, *72*, 031802.

(11) Hua, C. C.; Chen, C. L.; Chang, C. W.; Lee, C. K.; Chen, S. A. *J. Rheol.* **2005**, *49*, 641.

(12) Claudio, G. C.; Bittner, E. R. J. *Chem. Phys.* **2001**, *115*, 9585.

(13) Kumar, P.; Mehta, A.; Mahurin, S. M.; Dai, S.; Dadmun, M. D.; Sumpter, B. G.; Barnes, M. D. *Macromolecules* **2004**, *37*, 6132.

(14) Sumpter, B. G.; Kumar, P.; Mehta, A.; Barnes, M. D.; Shelton, W. A.; Harrison, R. J. *J. Phys. Chem. B* **2005**, *109*, 7671.
(15) Shie, S. C; Hua, C. C.; Chen, S. A *Macromol. Theory Simul.* **2007**, *16*, 111.
(16) Fukunaga, H.; Takimoto, J. I.; Doi, M. *J. Chem. Phys.* **2002**, *16*, 8183.
(17) Müller-Plathe, F. *ChemPhysChem* **2002**, *3*, 754.
(18) Chang, R.; Yethiraj, A. *J. Chem. Phys.* **2001**, *114*, 7688.
(19) Liu, C.; Muthukumar, M. *J. Chem. Phys.* **1998**, *109*, 2536.
(20) Tschöp, W.; Kremer, K.; Batoulis, J.; Bürger, T.; Hahn, O *Acta Polym.* **1998**, *49*, 61.
(21) Abrams, C. F.; Kremer, K. *Macromolecules* **2003**, *36*, 260.
(22) Clancy, T. C. *Polymer* **2004**, *45*, 7001.
(23) Faller, R.; Müller-Plathe, F. *Polymer* **2002**, *43*, 621.
(24) Faller, R. *Polymer* **2004**, *45*, 3869.
(25) Li, X.; Ma, X.; Huang, L.; Liang, H. *Polymer* **2005**, *46*, 6507.
(26) Li, X.; Kou, D.; Rao, S.; Liang, H. *J. Chem. Phys.* **2006**, *124*, 204909_1.
(27) Reith, D.; Meyer, H.; Müller-Plathe, F. *Macromolecules* **2001**, *34*, 2335.
(28) Boek, E. S.; Padding, J. T.; den Otter, W. K.; Briels, W. J. *J. Phys. Chem. B* **2005**, *109*, 19851.
(29) Marrink, S. J.; de Vries, A. H.; Mark, A. E. *J. Phys. Chem. B* **2004**, *108*, 750.
(30) Shelley, J. C.; Shelly, M. Y.; Reeder, R. C.; Bandyopadhyay, S.; Klein, M. L. *J. Phys. Chem. B* **2001**, *105*, 4464.
(31) Shih, A. Y.; Arkhipov, A.; Freddolino, P. L.; Schulten, K. *J. Phys. Chem. B* **2006**, *110*, 3674.
(32) Forester, T. R.; Smith, W. *The DL_POLY_2 Reference Manual*; Daresbury Laboratory; Daresbury, U.K., 2006.
(33) Mayo, S.; Olafson, B.; Goddard, W. *J. Phys. Chem.* **1990**, *94*, 8897.
(34) Allen, M. P.; Tildesley, D. J. *Computer Simulations of Liquids*; Oxford: Clarendon, U.K., 1990.
(35) Landau, D. P.; Binder, K. *A Guide to Monte Carlo Simulations in Statistical Physics*; Cambridge: New York, 2001.
(36) Kumar, S.; Larson, R. G. *J. Chem. Phys.* **2001**, *114*, 6937.
(37) Pamies, R.; Lopez Martinez, M. C.; Hernandez Cifre, J. G.; de la Torre, J. G. *Macromolecules* **2005**, *38*, 1371.
(38) Doi, M.; Edwards, S. F. *The Theory of Polymer Dynamics*; Oxford: New York, 1986.
(39) Dünweg, B.; Kremer, K. *J. Chem. Phys.* **1993**, *99*, 6983.
(40) Öttinger, H. C. *J. Non-Newtonian Fluid Mech.* **2004**, *120*, 207.
(41) Gettinger, C. L.; Heeger, A. J.; Drake, J. M.; Pine, D. J. *J. Chem. Phys.* **1994**, *101*, 1673.
(42) Banaszak, B. J.; de Pablo, J. J. *J. Chem. Phys.* **2003**, *119*, 2456.
(43) Brûlet, A.; Boué, F.; Cotton, J. P. *J. Phys. II Fr.* **1996**, *6*, 885.
(44) The independence check performed here has been motivated by the suggestion of an anonymous reviewer; moreover, the reviewers' comments have led us to identify the spurious flexibilities associated with one of the CG models considered in this figure (i.e., filled squares).

JP077054G